EDGE ARTICLE

Check for updates

Redox and photocatalytic properties of a Ni^II complex with a macrocyclic biquinazoline (Mabiq) ligand†‡

Michael Grübel, Irene Bosque, Philipp J. Altmann, Thorsten Bach (iD) *
and Corinna R. Hess (iD) *

We present a late, first row transition metal photosensitizer that promotes photocatalytic C–C bond formation. The title compound, [Ni(Mabiq)]OTf, as well as its one-electron reduced form, Ni(Mabiq), were synthesized and molecular structures of both were obtained. The electronic structure of the reduced complex additionally was characterized by spectroscopic and DFT computational methods. Notably, [Ni^II(Mabiq)]OTf is photoactive: reduction of the compound was achieved photochemically upon irradiation at $\lambda = 457$ nm and reductive quenching by NEt_3. The performance of [Ni(Mabiq)]OTf as a photoredox catalyst was examined in the cyclization of a bromoalkyl-substituted indole. In this reaction, the first-row transition metal compound is comparable if not superior to $[Ru(bpy)_3]^{2+}$ in terms of efficiency (turnover number) and chemoselectivity. Studies using a series of sacrificial donor amines indicate that the excited state redox potential of $[Ni(Mabiq)]^{+*}$ is ≥ 1.25 V *vs.* SCE. This value is similar to the excited state potential of commonly employed noble metal based photocatalysts. The Ni-Mabiq compound thus provides a rare example of an earth-abundant photoredox catalyst.

Introduction

Photoredox catalysis offers nascent opportunities to shift conventional chemical production methods to light-driven processes.[1] The design of new photoactive metal compounds is key to the development of new catalytic transformations. Chromophores can effect a wide array of functional group transformations and C–C bond formation reactions *via* the generation of active radical species, originating from excited state electron transfer processes (Scheme 1).[2] With very few exceptions, photoredox catalysis relies on the use of noble metal containing photosensitizers, mainly Ru- or Ir-polypyridyl complexes;[3] other heavy metal complexes (*e.g.* Os^II, Re^I, Mo^0, W^0) also have occasionally been employed.[4,5] $[Ru(bpy)_3]^{2+}$ – with its long lived, charge separated excited state $([Ru^{III}(bpy^{\cdot-})(bpy)_2]^{2+*})$ – is the classic and universal photocatalyst for a plethora of applications.[2]

The use of less expensive, more abundant, late first row transition metal alternatives is generally precluded by their inherently short excited-state lifetimes. In the first row, nickel complexes have been used in photocatalytic cross coupling reactions,[6] though the use of an added photosensitizer (commonly Ir) still is required in all of these tandem systems. A class of Ni^II ligand-to-ligand charge transfer complexes recently were shown to possess advantageous properties as photosensitizers, but applications have not yet been demonstrated.[7] In fact, reports describing catalytic applications or reactivity of systems using only non-noble metal photosensitizers are exceedingly scarce.[8–10]

Scheme 1 Photoredox catalysis commonly relies on noble metal complexes for organic transformations, initiated by single electron transfer upon excitation of Ru or Ir compounds. The [Ni(Mabiq)]OTf catalyst offers an earth-abundant photosensitizer.

Department of Chemistry, Catalysis Research Center (CRC), Technische Universität München, 85747 Garching, Germany. E-mail: thorsten.bach@ch.tum.de; corinna.hess@ch.tum.de

† Dedicated to the memory of Inge Grübel.

‡ Electronic supplementary information (ESI) available: CIF files, synthetic procedures, spectroscopic, electrochemical and DFT computational data. CCDC 1538675, 1538676 and 1586948. For ESI and crystallographic data in CIF or other electronic format see DOI: 10.1039/c7sc05320g

We now report a Ni^{II} complex with a macrocyclic biquinazoline (Mabiq) ligand,[11,12] [Ni(Mabiq)]OTf (1), providing a rare example of a non-noble metal based photosensitizer. The divalent complex 1 can be photochemically reduced and the electronic structure of the product, [Ni(Mabiq)] (2), is described herein. Using a series of synthesized sacrificial donor molecules, the photo-excited state redox potential of 1 was assessed and compared to common noble-metal photocatalysts. We demonstrate the photoredox catalytic ability of 1 in a radical-based cyclization of a bromoalkyl-substituted indole. The reaction relies solely on the Ni-Mabiq photocatalyst, without the need for an additional noble metal photosensitizer.

Results and discussion

The yellow diamagnetic 1 (Scheme 2) was readily prepared by complexation of the ligand with Ni(OTf)$_2$ in ethanol solution (see ESI‡ for further details). The Ni ion adopts the expected square planar geometry in the solid state (Fig. S1‡). The electronic spectrum of 1 in DCM exhibits intense absorption bands ($\varepsilon \approx 10^4$ M^{-1} cm^{-1}) in the visible light region ($\lambda_{max} = 414, 435$, and 457 nm; $\varepsilon = 13.6, 16.4, 22.3 \times 10^3$ M^{-1} cm^{-1}; Fig. 2 inset). Similar features were observed in the spectra of other M-Mabiq complexes, notably in the spectrum of Zn(Mabiq)Cl.[12a] The Zn^{II}-complex displayed two strong absorption bands at 471 and 502 nm that were assigned as Mabiq $\pi \rightarrow \pi^*$ transitions. However, d–d or metal-to-ligand charge transfer (MLCT) processes may additionally contribute to the corresponding absorptions of 1. The cyclic voltammogram of 1 in MeCN (Fig. S9‡) exhibits a reversible, formally Ni$^{II/I}$ redox couple at −1.05 V vs. Fc$^{+/0}$ (Fc = ferrocene; Fc$^{+/0} = 0.4$ V vs. SCE). Additional, seemingly reversible, reductive processes appear at potentials <−1.5 V.

The one-electron reduced Ni(Mabiq) (2) was subsequently generated from 1 using CoCp$_2$ as the reductant (Scheme 2). The molecular structure of 2 (Fig. 1) reveals shorter Ni–N bond distances (Ni–N$_{avg} = 1.874$ Å vs. Ni–N$_{avg} = 1.882$ Å in 1), as well as the hallmark changes in the diketiminate C–N bonds that signify reduction of the Mabiq ligand (Table S8‡). The $S = 1/2$ ground state of the complex was verified by EPR spectroscopy. The spectrum is consistent with a ligand-centered radical, with $g_{iso} = 1.995$ (Fig. S4‡). Low energy features at $\lambda_{max} = 641, 711$ and 801 nm (1.4, 3.5, 5.4 × 10^3 M^{-1} cm^{-1}) are apparent in the electronic spectrum of 2 in THF (Fig. 2 inset), accounting for the

Fig. 1 Left: Molecular structure of 2 (50% probability ellipsoids; hydrogen atoms omitted for clarity). Right: DFT-derived (B3LYP) spin density plot for 2 based on Löwdin population analysis (isosurface value = ±0.005).
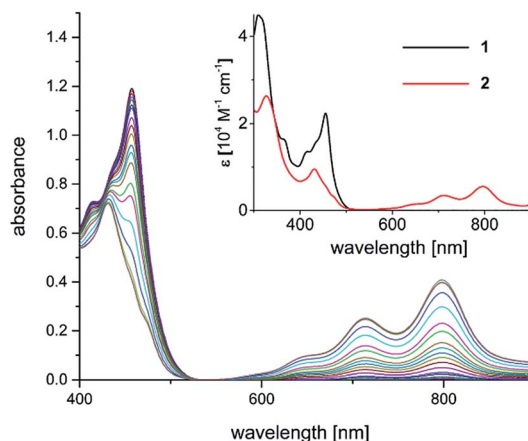

Fig. 2 Spectral evolution during photoconversion of 1 to 2 [c (1) = 0.05 mM; c (NEt$_3$) = 1.4 M; λ = 457 nm, DMF]. Inset: electronic spectra of 1 (black trace; CH$_2$Cl$_2$) and 2 (red trace; THF).

vibrant green color of the complex in solution. The spectrum again closely resembles that of the one-electron reduced Zn complex, Zn^{II}(Mabiq$^{\bullet-}$).[12a] The spectroscopic data thus point to ligand-centered reduction of 1, such that the electronic structure of 2 corresponds to Ni^{II}(Mabiq$^{\bullet-}$). Indeed, DFT calculations (B3LYP) on 2 further support this conclusion.

The DFT-derived (B3LYP) spin density plot (Fig. 1) describes a diamagnetic d^8 Ni^{II} center with an unpaired electron localized primarily on the diketiminate unit of the Mabiq ligand. Four doubly occupied d-orbitals can be identified, while the SOMO possesses only ca. 4% d-orbital character and otherwise depicts a ligand π^* orbital (Fig. S5‡). The latter molecular orbital is antibonding with respect to the diketiminate C–N p-orbital interactions, which explains the lengthening of these bonds in the structure of 2. It is noteworthy that ligand-centered reduction appears to prevail across the series of metal-Mabiq compounds we have examined thus far.[12]

The well-behaved redox chemistry of [Ni(Mabiq)]OTf (1), its high absorbance in the visible region and its relatively high reduction potential warranted a study of its photoredox properties. As mentioned above, the compound exhibits a strong

Scheme 2 Reaction of 1 with CoCp$_2$ (Cp = cyclopentadienyl) yields the one-electron reduced 2.

multi-structured absorption band with a maximum at $\lambda = 457$ nm ($\varepsilon = 22\,300$ M^{-1} cm^{-1}), which invites excitation with a visible light source and quenching studies with a suitable reductant. Gratifyingly, it was indeed found that irradiation of a DMF solution of **1** at $\lambda = 457$ nm, in the presence of NEt$_3$ (7.5 mM to 1.4 M), leads to a color change from yellow to green and to the formation of complex **2**.

The formation of the reduced compound was complete after 15 minutes (using 1.4 M NEt$_3$; c (**1**) = 0.05 mM), as verified spectroscopically (Fig. 2). The photoconversion of **1** to **2** occurs on a much faster timescale in MeCN/THF or DMF/THF mixtures (the solvent combination solubilizes both forms), under identical conditions. The quantum yield for the photoconversion is $\approx 10^{-4}$ (THF : DMF 4 : 1), and correlates with the Et$_3$N concentration (14–56 mM; Table S3 and Fig. S29‡). From the data, the lifetime of the excited state form that reacts with the Et$_3$N can be estimated as $\approx 1 \times 10^{-8}$ s (see ESI‡ for details). Steady-state emission spectra recorded at ambient temperature and at 77 K did not reveal any luminescence. Thus, we currently cannot comment in detail on the nature of the excited state processes involved in the photo-reduction of **1**. If one takes the longest wavelength absorption [$\lambda \cong 510$ nm, $E_0 \le 235$ kJ mol^{-1} (2.4 V)] of compound **1** to estimate the redox potential of photoexcited complex **1***, a value of $\le +1.35$ V ($vs.$ Fc$^{+/0}$) is obtained.[13]
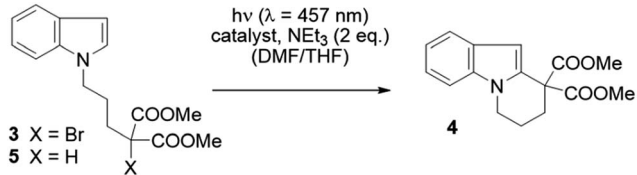
TDDFT (B3LYP) computational studies provide some insight into the nature of the absorptions in the visible region. The calculated transitions correlate well with the experimentally obtained absorbance spectrum of **1** (Fig. S6‡). The absorptions at 400–500 nm include a prominent LL'CT transition that corresponds to the HOMO to LUMO transition. The HOMO is localized on the bipyrimidine moiety of the Mabiq ligand, while the LUMO is a diketiminate based π^* orbital (Fig. S7‡). Other, less intense, transitions in the vicinity possess d–d (Ni d$_{z^2}$ → Ni d$_{x^2-y^2}$) and MLCT (Ni d$_{z^2}$ → L$_{\pi^*}$) character. These states may contribute to the unique photochemical properties of **1**. However, a detailed investigation regarding the photochemistry and excited state kinetics of this compound is warranted, and will be the subject of future investigations.

We examined whether the photochemical properties of **1** might render it a suitable photoredox catalyst for C–C bond formation reactions. The radical cyclization of the N-(ω-bromoalkyl)-substituted indole **3** was chosen as a test reaction.[14] The reaction had been previously studied by the Stephenson group and was found to produce mainly product **4** by C–C bond formation under optimized conditions.[15] Under non-optimized conditions, hydro-de-bromination was a competing side reaction and varying product ratios of **4** and **5** were observed. Optimal conditions were reported to include the use of [Ru(bpy)$_3$]Cl$_2$ as the catalyst (1 mol%) and NEt$_3$ (2 equiv.) in DMF solution and gave product **4** in 60% yield.[15]

Given the limited solubility of **2** in DMF, the reaction was initially attempted in a DMF/THF mixture (v/v = 1/2) with 2 mol% of catalyst **1** and 2 equiv. NEt$_3$ as the quencher (Table 1, entry 1).[16] We were pleased to find that the desired cyclization proceeded smoothly and delivered with high chemoselectivity the desired product **4**. The inseparable hydro-de-brominated by-product **5** was detectable in minor quantities but the ratio of products was 95/5 in favor of cyclization product **4**. When increasing the relative volume of THF in the solvent mixture both conversion and yield improved slightly (entry 2). The selectivity towards the desired reaction was high with a yield of 86% at 94% conversion, $i.e.$ 91% yield based on conversion. For comparison, the Ru^{II} complex [Ru(bpy)$_3$](PF$_6$)$_2$ was employed under identical conditions (entry 3). Although the ratio **4/5** was identical with this catalyst, the reaction suffered from a lower conversion and a lower chemoselectivity (63% yield based on conversion). Similar observations were made when the catalyst

Table 1 Photoredox-catalyzed cyclization of bromide **3** to tricyclic product **4** and reduction to hydro-de-brominated product **5**; influence of the catalyst and the reaction parameters on the yield and chemoselectivity

Entry[a]	Catalyst[a]	mol%	DMF/THF [v/v]	Conv.[b] [%]	Yield[c] [%]	**4/5**[d]
1	**1**	2	1/2	93	84	95/5
2	**1**	2	1/4	94	86	95/5
3	[Ru(bpy)$_3$](PF$_6$)$_2$	2	1/4	73	46	95/5
4	**1**	1	1/4	95	84	95/5
5	[Ru(bpy)$_3$](PF$_6$)$_2$	1	1/4	59	23	95/5
6	**1**[e]	2	1/4	n.d.	—	—
7	—[f]	—	1/4	12	12	55/45
8	**1**[g]	2	1/4	<5	<5	—

[a] All reactions were performed on a scale of 0.08 mmol (c = 25 mM) with a LED lamp (3 W power output) as light source. Irradiation time: 13 h. [b] The conversion was calculated from recovered starting material. [c] Total yield of isolated products **4** and **5**. [d] Ratio of cyclized to hydro-de-brominated product as determined by ^{1}H-NMR. [e] Attempted reaction without irradiation. [f] No catalyst was added. [g] No NEt$_3$ was added. n.d. = not detected.

loading was further decreased to 1 mol%: while the performance of Ni^{II} catalyst **1** remained unchanged (entry 4) the reaction with the Ru^{II} catalyst was sluggish and a decrease in yield was observed (entry 5).

The above reaction is induced by visible light as no conversion occurs without irradiation (entry 6). In the absence of the Ni^{II} catalyst,[17] only 12% of a product mixture was obtained, which was composed of the cyclized product **4** and the reduced product **5** in a 55/45 ratio (entry 7). In the absence of the reductant, no reaction was observed (entry 8). The free HMabiq ligand is not photocatalytically active. The quantum yield for the [Ni(Mabiq)]OTf catalysed cyclization reaction was determined to be $\Phi = 0.006$.

Mechanistically, it is suggested that the photoreduction of complex **1** by NEt$_3$ (reductive quenching cycle)[1] generates complex **2**, which may engage in SET to the bromide **3** (Scheme 3). Complex **2** was shown to be competent to reduce **3**. We note that modification of the Ni-Mabiq complex during the cyclization reaction was not observed, as verified by ESI-MS and ^{1}H-NMR (Fig. S8 and S41‡).

To experimentally verify the estimated photoexcited state redox potential of **1***, we synthesized a series of amines with oxidation potentials in the range of 0.78–1.59 V (*vs.* SCE; Tables 2 and S1‡), as determined by CV. The amines were employed as sacrificial donors in the cyclization reaction. Excellent yields of **4** were obtained using the donor molecules with oxidation potentials up to 1.25 V (Table 2, amines **6a**–**6c**), whereas a drastic decrease in yield was observed using those with higher redox potentials. Only 40% and 20% product yields were obtained with **6d** ($E_{ox} = 1.41$ V *vs.* SCE) and **6e** ($E_{ox} = 1.59$ V *vs.* SCE), respectively. The product yield in the control reaction using **6e** in the absence of photocatalyst **1** was 7%, a result that is comparable to that obtained using NEt$_3$ (Table 1, entry 7). The results confirm that the excited state redox potential of **1*** is at least 1.25 V (*vs.* SCE). Thus, our new Ni-Mabiq complex is a more powerful oxidant than [Ru(bpy)$_3$]$^{2+}$ ($E_{1/2}$ [Ru^{2+}*/Ru$^+$] 0.78 V *vs.* SCE),[18] and comparable to [Ir(dF(CF$_3$)ppy)$_2$(dtbbpy)]$^+$ ($E_{1/2}$ [Ir^{3+}*/Ir^{2+}] 1.21 V *vs.* SCE).[19]

We additionally generated a sterically hindered amine, N(CH$_2$Mes)Cy$_2$ (**6f**), to assess whether coordination of the sacrificial donor molecules influences the reactivity of **1**. In contrast to the bpy- and phen-based photosensitizers, the Ni-Mabiq complexes are coordinatively unsaturated and intramolecular electron transfer from a coordinated amine to the

Table 2 Comparison of the oxidation potentials for different sacrificial donors **6** with the yields obtained for the catalytic reaction of **3** to **4** and **5**

Amine^a	E_{ox} (*vs.* SCE)	Yield^b [%]
Et$_3$N (**6a**)	0.83	84
6b	1.05	97
6c	1.25	95
6d	1.41	40
6e	1.59	20^c
6f	0.78	84

^{a} All reactions were performed on a scale of 0.08 mmol ($c = 25$ mM) with a 457 nm LED lamp (3 W power output) as the light source. Irradiation time: 13 h. ^{b} Total yield of isolated products **4** and **5**, with a 95 : 5 ratio of cyclized to hydro-de-brominated product as determined by ^{1}H-NMR. ^{c} Average of two runs. Fc$^{+/0}$ = 0.4 V *vs.* SCE. Cy = cyclohexyl.

divalent metal center could potentially occur. The molecular structure of **6f** (Fig. S3‡) suggests that coordination of this amine group to the Ni center is unlikely; the cyclohexyl and mesityl groups encapsulate the nitrogen atom rendering the lone pair inaccessible. Whereas noticeable changes in the absorption spectrum of **1** were observed upon addition of Et$_3$N (400 equiv.) to a solution of the complex in THF/DMF, the addition of **6f** has no effect (Fig. S30 and S31‡). However, the yield of the catalytic reaction using **6f** as sacrificial donor was found to be 84%, a value that is comparable to the one obtained using Et$_3$N (**6a**) and **6b**–**6e** as sacrificial donors.

Conclusions

In summary, we have discovered a new photoredox catalyst, [Ni(Mabiq)]OTf (**1**) that is based on the earth-abundant metal nickel. The diamagnetic, bench-stable compound was readily prepared, its redox properties were studied and the one-electron reduced form Ni(Mabiq) (**2**) likewise was isolated. Further studies to elucidate the detailed photophysical properties of **1*** are warranted. However, we have already demonstrated that the photoexcited complex is a strong oxidant, with the capacity to induce C–C bond formation in an initial test reaction. The Ni-Mabiq compound may offer an alternative to noble metal photosensitizers for other synthetic transformations in organic photoredox chemistry, as well as for energy conversion processes. The Mabiq ligand also features a second metal binding site that could be exploited for tandem catalysis. Thus, the macrocycle represents a new type of platform for the development of photoactive systems. With evidence of the ability of **1** to act as a photosensitizer and photoredox catalyst, the broader photocatalytic applications of our system subsequently will be investigated.

Scheme 3 Proposed catalytic cycle for the cyclization of **3** to give **4**.

Conflicts of interest

There are no conflicts to declare.

Acknowledgements

Notes and references

1 For seminal studies, see: (a) M. A. Ischay, M. E. Anzovino, J. Du and T. P. Yoon, *J. Am. Chem. Soc.*, 2008, **130**, 12886–12887; (b) D. A. Nicewicz and D. W. C. MacMillan, *Science*, 2008, **322**, 77–80; (c) J. M. R. Narayanam, J. W. Tucker and C. R. J. Stephenson, *J. Am. Chem. Soc.*, 2009, **131**, 8756–8757.

2 Reviews: (a) D. M. Schultz and T. P. Yoon, *Science*, 2014, **343**, 985; (b) Y. Xi, H. Yi and A. Lei, *Org. Biomol. Chem.*, 2013, **11**, 2387–2403; (c) M. Reckenthäler and A. G. Griesbeck, *Adv. Synth. Catal.*, 2013, **355**, 2727–2744; (d) C. K. Prier, D. A. Rankic and D. W. C. MacMillan, *Chem. Rev.*, 2013, **113**, 5322–5363; (e) J. M. R. Narayanam and C. R. J. Stephenson, *Chem. Soc. Rev.*, 2011, **40**, 102–113; (f) K. Zeitler, *Angew. Chem., Int. Ed.*, 2009, **48**, 9785–9789.

3 D. M. Arias-Rotondo and J. K. McCusker, *Chem. Soc. Rev.*, 2016, **45**, 5803–5820.

4 (a) L. A. Büldt and O. S. Wenger, *Angew. Chem., Int. Ed.*, 2017, **56**, 5676–5682; (b) L. A. Büldt, X. Guo, A. Prescimone and O. S. Wenger, *Angew. Chem., Int. Ed.*, 2016, **55**, 11247–11250; (c) J.-P. Sauvage, J.-P. Collin, J.-C. Chambron, S. Guillerez and C. Coudret, *Chem. Rev.*, 1994, **94**, 993–1019; (d) D. J. Stufkensa and A. Vlcek Jr, *Coord. Chem. Rev.*, 1998, **177**, 127–179; (e) K. S. Schanze, D. B. MacQueen, T. A. Perkins and L. A. Cabana, *Coord. Chem. Rev.*, 1993, **122**, 63–89; (f) S. Meister, R. O. Reithmeier, M. Tschurl, U. Heiz and B. Rieger, *ChemCatChem*, 2015, **7**, 690–697.

5 For the use of organic compounds as photoredox catalysts, see: N. A. Romero and D. A. Nicewicz, *Chem. Rev.*, 2016, **116**, 10075–11166.

6 (a) Z. Zuo, D. T. Ahneman, L. Chu, J. A. Terrett, A. G. Doyle and D. W. C. MacMillan, *Science*, 2014, **345**, 437–440; (b) D. T. Ahneman and A. G. Doyle, *Chem. Sci.*, 2016, **7**, 7002–7006; (c) M. Jouffroy, D. N. Primer and G. A. Molander, *J. Am. Chem. Soc.*, 2016, **138**, 475–478; (d) B. P. Woods, M. Orlandi, C.-Y. Huang, M. S. Sigman and A. G. Doyle, *J. Am. Chem. Soc.*, 2017, **139**, 5688–5691; (e) M. K. Nielsen, B. J. Shields, J. Liu, M. J. Williams, M. J. Zacuto and A. G. Doyle, *Angew. Chem., Int. Ed.*, 2017, **56**, 7191–7194; (f) J. Twilton, C. Le, P. Zhang, M. H. Shaw, R. W. Evans and D. W. C. MacMillan, *Nat. Rev. Chem.*, 2017, **1**, 1–18; (g) E. R. Welin, C. Le, D. M. Arias-Rotondo, J. K. McCusker and D. W. C. MacMillan, *Science*, 2017, **355**, 380–385.

7 L. A. Cameron, J. W. Ziller and A. F. Heyduk, *Chem. Sci.*, 2016, **7**, 1807–1814.

8 For a recent review of earth-abundant photosensitizers see: C. B. Larsen and O. S. Wenger, *Chem.–Eur. J.*, 2018, **24**, 2039–2058.

9 (a) F. J. Sarabia and E. M. Ferreira, *Org. Lett.*, 2017, **19**, 2865–2868; (b) S. M. Stevenson, M. P. Shores and E. M. Ferreira, *Angew. Chem., Int. Ed.*, 2015, **54**, 6506–6510; (c) A. Gualandi, M. Marchini, L. Mengozzi, M. Natali, M. Lucarini, P. Ceroni and P. G. Cozzi, *ACS Catal.*, 2015, **5**, 5927–5931; (d) P. Zimmer, P. Müller, L. Burkhardt, R. Schepper, A. Neuba, J. Steube, F. Dietrich, U. Flörke, S. Mangold, M. Gerhards and M. Bauer, *Eur. J. Inorg. Chem.*, 2017, 1504–1509; (e) S. Otto, A. M. Nauth, E. Ermilov, N. Scholz, A. Friedrich, U. Resch-Genger, S. Lochbrunner, T. Opatz and K. Heinze, *ChemPhotoChem*, 2017, **1**, 344–349.

10 S. J. Hwang, D. C. Powers, A. G. Maher, B. L. Anderson, R. G. Hadt, S.-L. Zheng, Y.-S. Chen and D. G. Nocera, *J. Am. Chem. Soc.*, 2015, **137**, 6472–6475.

11 E. Müller, G. Bernardinelli and A. von Zelewsky, *Inorg. Chem.*, 1988, **27**, 4645–4651.

12 (a) P. Banerjee, A. Company, T. Weyermüller, E. Bill and C. R. Hess, *Inorg. Chem.*, 2009, **48**, 2944–2955; (b) E. V. Puttock, P. Banerjee, M. Kaspar, L. Drennan, D. S. Yufit, E. Bill, S. Sproules and C. R. Hess, *Inorg. Chem.*, 2015, **54**, 5864–5873; (c) M. Kaspar, P. J. Altmann, A. Pöthig, S. Sproules and C. R. Hess, *Chem. Commun.*, 2017, **53**, 7282–7285.

13 The redox potential of **1***/**2** was calculated from the redox potential of **1**/**2** (−1.05 V *vs.* Fc$^{+/0}$) by adding the energy of the excited state E_0 (see ref. 3).

14 For recent work on photoredox-induced alkylation reactions at the indole core, see: D. Alpers, M. Gallhof, J. Witt, F. Hoffmann and M. Brasholz, *Angew. Chem., Int. Ed.*, 2017, **56**, 1402–1406 and refs cited therein.

15 J. W. Tucker, J. M. R. Narayanam, S. W. Krabbe and C. R. J. Stephenson, *Org. Lett.*, 2010, **12**, 368–371.

16 For the reaction set-up, see: (a) D. Rackl, V. Kais, P. Kreitmeier and O. Reiser, *Beilstein J. Org. Chem.*, 2014, **10**, 2157–2165; (b) D. Lenhart, A. Pöthig and T. Bach, *Chem.–Eur. J.*, 2016, **22**, 6519–6523.

17 Radical reactions of amines can be initiated in the absence of a photoredox catalyst if an alkyl halide is present: (a) J. F. Franz, W. B. Kraus and K. Zeitler, *Chem. Commun.*, 2015, **51**, 8280–8283; (b) A. Böhm and T. Bach, *Chem.–Eur. J.*, 2016, **22**, 15821–15928; (c) A. M. Nauth, J. C. O. Pacheco, S. Pusch and T. Opatz, *Eur. J. Org. Chem.*, 2017, 6966–6974.

18 A. Juris, V. Balzani, P. Belser and A. von Zelewsky, *Helv. Chim. Acta*, 1981, **64**, 2175–2182.

19 M. S. Lowry, J. I. Goldsmith, J. D. Slinker, R. Rohl, R. A. Pascal Jr, G. G. Mailliaras and S. Bernhard, *Chem. Mater.*, 2005, **17**, 5712–5719.